Toxicology Letters 265 (2017) 77–85

Contents lists available at ScienceDirect

Toxicology Letters

journal homepage: www.elsevier.com/locate/toxlet

Toxicokinetics of titanium dioxide (TiO_2) nanoparticles after inhalation in rats

Igor Pujalté[a], Denis Dieme[a], Sami Haddad[a], Alessandra Maria Serventi[b], Michèle Bouchard[a,*]

[a] Department of Environmental and Occupational Health, Chair in Toxicological Risk Assessment and Management, and University of Montreal Public Health Research Institute (IRSPUM), University of Montreal, Roger-Gaudry Building, U424, P.O. Box 6128, Main Station, Montreal, Quebec, H3C 3J7, Canada
[b] Institute of Research of Hydro-Quebec (IREQ), 1800, Boul. Lionel-Boulet, Varennes, Québec, J3X 1S1, Canada

HIGHLIGHTS

- The kinetics of TiO_2 nanoparticles was studied in rats after a 6-h inhalation.
- TiO_2 persisted in lungs, where highest tissue levels were found.
- TiO_2 in lungs reached peak values only at 48 h and levels decreased over 14 days.
- Fecal amounts suggest a mucociliary clearance of inhaled NPs and ingestion.
- A certain translocation to the olfactory bulb and the brain was also observed.

ARTICLE INFO

Article history:
Received 18 July 2016
Received in revised form 20 October 2016
Accepted 20 November 2016
Available online 22 November 2016

Keywords:
Titanium dioxide nanoparticles
Toxicokinetics
Inhalation
Rats

ABSTRACT

This study focused on the generation of aerosols of titanium dioxide (TiO_2) nanoparticles (NPs) and their disposition kinetics in rats. Male Sprague-Dawley rats were exposed by inhalation to 15 mg/m^3 of anatase TiO_2 NPs (~20 nm) during 6 h. Rats were sacrificed at different time points over 14 days following the onset of inhalation. Ti levels were quantified by ICP-MS in blood, tissues, and excreta. Oxidative damages were also monitored (MDA). Highest tissue levels of Ti were found in lungs; peak values were reached only at 48 h followed by a progressive decrease over 14 days, suggesting a persistence of NPs at the site-of-entry. Levels reached in blood, lymph nodes and other internal organs (including liver, kidney, spleen) were *circa* one order of magnitude lower than in lungs, but the profiles were indicative of a certain translocation to the systemic circulation. Large amounts were recovered in feces compared to urine, suggesting that inhaled NPs were eliminated mainly by mucociliary clearance and ingested. TiO_2 NPs also appeared to be partly transferred to olfactory bulbs and brain. MDA levels indicative of oxidative damage were significantly increased in lungs and blood at 24 h but this was not clearly reflected at later times. Translocation and clearance rates of inhaled NPs under different realistic exposure conditions should be further documented.

1. Introduction

Titanium dioxide (TiO_2) nanoparticles (NPs) are among the most produced NPs in the world. They have been widely used in consumer and industrial products due to their unique physical and chemical properties (Berube et al., 2010; Shi et al., 2013). Human exposure to NPs can occur during manufacture or use of nanostructured products. Inhalation and dermal contact are considered as potential routes of exposure in workers (Berges, 2013; Kuhlbusch et al., 2011). However, there is currently no significant evidence for NP uptake through the intact skin (Shi et al., 2013). On the other hand, inhaled NPs are described as being able to reach the deep lung and to deposit in the alveolar regions; maximum distribution size of the deposited NPs were found to be between 10 and 100 nm (Hinds, 1999). In some studies, little retention and systemic absorption of deposited NPs have been

* Corresponding author at: Department of Environmental and Occupational Health University of Montreal Roger–Gaudry Building, Room U424, P.O. Box 6128, Main Station, Montreal, Quebec, H3C 3J7, Canada.
E-mail address: michele.bouchard@umontreal.ca (M. Bouchard).

http://dx.doi.org/10.1016/j.toxlet.2016.11.014
0378-4274/

reported with toxic effects mostly localized and limited to the lung (Bermudez et al., 2002; Landsiedel, 2013). Conversely, other studies suggest that NPs can cross the pulmonary barrier, reach the systemic circulation and thus have been shown to exert toxic damages in secondary organs (Iavicoli et al., 2012; Kreyling, 2013; Liang et al., 2009). The capacity to cross the lung barrier has been described as being size and concentration dependent (Geiser and Kreyling, 2010). The exact fraction of NPs that can reach the blood or lymphatic system is not well documented. Existing data suggest that the translocation fraction is in the order of 0.01 of total inhaled NPs (Kreyling, 2013). One hour after inhalation of 2–4 nm ^{192}Ir NPs by rats, Kreyling et al. (2009) observed that 0.1–1% of labelled dose was recovered in the liver, spleen, kidney, heart and brain and 1–5% were found in soft tissues and bones.

Following exposure to TiO_2 NPs more specifically at different concentration levels, some authors have reported hepatotoxic (Guo et al., 2009; Li et al., 2010), nephrotoxic (Chen et al., 2009; Zhao et al., 2010) and cardiotoxic effects (Liu et al., 2009). These target organs have been identified essentially following intravenous and intraperitoneal injection. Recently, Elgrabli et al. (2015) have focused on the biodistribution and clearance of intravenously administered TiO_2 NPs and found an accumulation of TiO_2 in liver primarily, followed by the spleen and lung, but there were no toxic effects (inflammation, biochemical markers, hispathological changes) identified at the high dose of 1.7 mg injected (7.7–9.4 mg/kg). However, these data do not take into consideration uptake through biological membranes and other aspects of toxicokinetic processes. Assessment following realistic exposure conditions such as inhalation is necessary.

Overall, there is thus a growing body of evidence on the potential toxicological effects of TiO_2 NPs based on *in vitro* and *in vivo* studies under certain exposure conditions (Pujalté et al., 2011; Shi et al., 2013). Nevertheless, for technical reasons, there are important knowledge gaps on the toxicokinetics of TiO_2 NPs, *i.e.* absorption/translocation, biodistribution and clearance, after the more relevant inhalation route of exposure. Inhalation facilities designed for "nose-only" NP exposure in animals are still rare. Compared to whole-body inhalation, it minimizes deposition of NPs on the animal's fur and potential indirect intake of NPs (Baisch et al., 2014; Yeh et al., 1990). Inhalation exposure is also preferred to intratracheal instillation because it allows to expose rats to small NP aerosols (Driscoll et al., 2000; Osier and Oberörster, 1997), reflects a more realistic route-of-exposure and avoids strong biological responses (inflammation, oxidative stress, lung overload) (Baisch et al., 2014). Noël et al. 2013a,b, 2012 set an inhalation system in our facilities to study inflammation in rat lungs following "nose-only" inhalation of different TiO_2 NP size and agglomeration states. Recently, a more optimized "nose-only" inhalation system was specifically designed and set up for different NP exposure conditions in our laboratory (Pujalté et al. submitted). The new inhalation system allows to generate nano-aerosols (<100 nm) stable through time. The objective of the current study was thus to assess the biodistribution of TiO_2 in blood, tissues and excretas over a 14-day period following a 6-h inhalation of nano-aerosols of the mostly used TiO_2 NPs (20 nm anatase). Exposure conditions aimed to reflect a typical daily exposure in workers and the selected NP initial size has been reported to favor deposition in the alveolus (Hinds, 1999) and hence translocation across membrane barriers.

2. Materials and methods

2.1. Animals

Male Sprague-Dawley rats weighing 150–175 g (5–6 weeks old) were purchased from Charles River (Charles River Canada Inc., St-Constant, Canada). Lighting was maintained on a 12-h light–dark cycle and room temperature was kept at 22 ± 5 °C. Prior to inhalation, the rats were placed two per cage and had access to water and food *ad libitum*. On days 1–6 prior to inhalation exposure, animals were progressively acclimatized to the "nose-only" inhalation units, thus during 15, 30, 45, 60, 180 and 360 min per day, respectively, to limit stress during exposure period. Over the 3 days preceding inhalation, they were also gradually acclimatized to the metabolic cages during 1, 2 and 3 h per day, respectively. Before exposure, a drop of mineral oil was deposited on their eyes to prevent irritation during exposure. Following inhalation period, rats were cleaned with a damp cloth to avoid indirect exposure with NPs and placed in individual metabolic cages (for separate collection of urine and feces). The weight gain for each animal was recorded daily. The experiment was approved by the Ethics Committee on Animal Experiments of the University of Montreal.

2.2. Aerosol generation and monitoring

TiO_2 NPs were purchased from Nanostructured & Amorphous Materials Inc. (Houston, Texas, USA). The manufacturer specifications indicated that the powdered material was composed of anatase TiO_2 (99%) with an average primary particle size between 10 and 30 nm and a specific surface area of 200–220 m^2/g. A NP suspension was prepared from NP powder in ultrapure deionized water (18 mΩ) at a concentration of 6.5 mg/mL and a constant stirring was applied (120 rpm for a 125 mL aqueous suspension).

A collision 6-jet aerosolizer (BGI Inc., Waltham, USA) was used for the generation of liquid aerosols (Hinds, 1999). The system uses compressed air at high velocity and a laminar separation compartment to generate fine aerosols for rat exposure (Pujalté et al. submitted). More specifically, a TiO_2 suspension is turbulently mixed with compressed purified air at high velocity to generate the aerosol. The generator operates at an airflow rate of 7.25 L/min and a maximum pressure of 2.76 bar (in a 0.5 L cylinder). The generated aerosol then passes through a diffusion dryer column composed of silica beads to remove water vapors. The dilution airflow rate with incoming compressed air is set by default at 20 L/min (in a 0.5 L cylinder). The aerosol then impacts against the inside of a laminar airflow glass vessel separator (370 cm^3) allowing to remove the larger fraction of particles. The remaining fine aerosols are directed to the rat exposure units (TSE Systems GmbH, Germany). The internal volume of the exposure chamber (4.9 L) was designed to simultaneously expose 30 rats "nose-only". Optimal exposure conditions for rats were monitored in this chamber, ensuring a sufficient airflow of 0.5 L/min/rat, optimal temperature of 22 °C, O_2 levels >19%, CO_2 levels <0.2% and a constant pressure (±−1 mbar). All experiments were performed in a ventilated safety glass cover (1.79 m^3), which allows protecting the personnel against direct exposure to NP aerosols.

A DustTrak Aerosol Monitor was used to estimate the mass concentration (mg/m^3) through time (Model 8520, TSI Inc., USA); values were recorded on line every 10 s and means, min and max were calculated over the total generation period. The time-integrated mass concentration of TiO_2 in the aerosol was calibrated by gravimetric analysis of a borosilicate glass filter of 50 mm (700–800-FI, TSE Systems GmbH, Germany) sampled at a flow rate of 2 L/min; a micro-balance (XP2U, Mettler-Toledo Inc., USA) was used to weigh the filter pre- and post-generation. The size distribution (nm) of the aerosol in the exposure chamber was also monitored on-line with a nanospectrometer (NanoSpectroPan, TSE Systems GmbH, Germany) equipped with 2 measurement units. The nanoparticle measuring unit uses an electrical sensor to monitor size in the electric mobility range of 10 to 193 nm and the optical aerosol measuring unit counts particles in the optical equivalence

diameter range of 0.250–35.2 μm. This device requires 1 min per scan at a sample flow rate of 1.2 L/min. The geometric mean diameter, d_g, and geometric standard deviation, σ_g, were used to determine the size distribution of particles in the aerosol based on the number of particles (particles/cm^3) (Hinds, 1999).

2.3. Rat inhalation exposure and biological sampling

Rats were exposed by inhalation to 15 mg/m^3 of TiO_2 NPs during 6 continuous hours. Controls were exposed to filtered air only. Animals were sacrificed by CO_2 asphyxiation. Blood was withdrawn by cardiac puncture and tissues (kidney, liver, spleen, pancreas, lungs, thymus, heart, lymph nodes, salivary glands, brain and olfactory bulbs) were excised at 0, 3, 6, 12, 24, 48, 72, 168 and 336 h (7 and 14 days) following the onset of inhalation. Six rats were used per time of sacrifice in the group exposed and the controls, except for the first three times where four rats per time point were used. Urine and feces were collected at times −24 to 0, 0–6, 6–12, 12–24 h and then daily over 14 days for the group of rats sacrificed on day 14. Blood was buffered with an equal volume of PBS buffer with 1 mM of ETDA (trace metal grade, 60-00-4, Sigma-Aldrich, Oakville, Canada) and 0.01% of butylated hydroxytoluene (128-37-0, Sigma-Aldrich, Oakville, Ontario, Canada), flash frozen in liquid nitrogen and stored at −80 °C until analysis. Tissue samples were rinced with saline at 0.9%, weighed, flash frozen in liquid nitrogen and stored at −80 °C until analysis, except for lymph nodes, olfactory bulbs, salivary glands, brain, thymus, heart, which were stored at −20 °C. Urine volume was measured and feces were weighed, and then stored at −20 °C until analysis.

2.4. Sample treatment and elemental ICP-MS analysis

Sample preparation and digestion for elemental titanium (Ti) analysis by ICP-MS was performed in a cleanroom (ISO 2 standards 146442-1). This wet digestion method used was adapted from Mester and Sturgeon (2003) and Subramanian, (2006). Briefly, tissues and feces collected were blended with a PBS buffer containing 1 mM of ETDA (trace metal grade, 60-00-4, Sigma-Aldrich, Oakville, Canada) and 0.01% of butylated hydroxytoluene (128-37-0, Sigma-Aldrich, Oakville, Ontario, Canada), at a final concentration of 0.250 mg/mL. Blood was directly diluted with PBS buffer, EDTA and butylated hydroxytoluene at a final concentration of 0.250 mg/mL and urine was not diluted. Then, 1 mL of sample was placed in a PFA digestion tube, spiked with internal standard of indium (In) (analytical grade, 00734, Fluka, Buchs, Switzerland) (final concentration of 1 μg/L), and homogenized with 3 mL of nitric acid (HNO_3) at 70% (trace metal grade, A509P212, Fisher Scientific, Ottawa, Canada), and 2 mL of hydrogen peroxide (H_2O_2) at 30% (optima grade, P170-500, Fisher Scientific, Ottawa, Canada). The mixture was digested overnight in a heating block (HotBlock sc150, Environmental Express, Charleston, USA) set to a maximum temperature of 135 °C. The solution was evaporated to a volume of less than 0.5 mL, and 0.25 mL of fluorhydric acid (HF) at 40% (optima grade, A463-5000, Fisher Scientific, Ottawa, Canada) and 2 mL of HNO_3 at 70% were added. The solution was evaporated to a volume of less than 0.25 mL with the block heater, readjusted to a volume of 10 mL with ultrapure deionized water (18 mΩ) and shortly shaken.

Elemental analysis was then conducted with an Agilent ICP-MS 7700x (Agilent, Mississauga, Canada) in a cleanroom (ISO 3 standards 146442-1). Quantification was carried out using a six-point-calibration curve with internal standard correction. All samples and standards were measured with the ICP-MS system operating in the following conditions: RF Power at 1600 W, nebulizer gas flow rate at 0.65 L of Ar/min, dilution gas flow rate of 0.4 L Ar/min, and collision gas flow of 4.5 mL He/min. The isotopes measured were ^{49}Ti and ^{115}In as internal standard. The limit of detection was in the order of 0.05 ppb, which is equivalent to 0.05 ng/g of tissue. Baseline values obtained from controls were subtracted from values observed in treated rats.

2.5. Characterization of the TiO_2 nanopowder, aerosols and lung tissue slices

The TiO_2 nanopowder used for inhalation exposure and the aerosol produced from TiO_2 suspension using the Collision-jet generator were characterized by scanning electron microscopy (SEM), transmission electron microscopy (TEM), selected area electron diffraction (SAD) and electron dispersive X-ray spectroscopy (EDX). This analysis was performed at the Material Characterization Laboratory of the Research Institute of Hydro-Québec. Initial analysis was conducted using a Hitachi SEM 4700 microscope and Hitachi H-9000 TEM. Material investigation was then carried out using a newly acquired performant microscope Hitachi HF 3300 E-TEM. This microscope allows to observe a large variety of materials at different temperatures, under vacuum conditions or in a gas atmosphere. It is equipped with conventional and high resolution imaging modes, electron diffraction modes (selected area electron diffraction and nano-diffraction mode), electron dispersive X-ray spectroscopy (EDX of Gatan) and electron energy loss spectroscopy (EELS of Gatan).

The original TiO_2 nanopowder was observed by SEM and TEM, and the corresponding SAD was determined to confirm its composition and structural phase. TEM images of NPs dispersed in the aerosol and collected on a typical TEM grid placed in the inhalation chamber in lateral position were also taken; a typical TEM grid is made of an amorphous carbon hole film placed on a Cu grid disc.

Slices of rat lungs collected 6 h post-exposure were further observed by TEM, after preparation performed by the Histology Platform Laboratory of Sherbrooke University. Briefly, after sampling and fixation, the lung was cut in thin slices by ultramicrotomy using a Pb and/or uranyl acetate coloration. The lung slices were then placed on Cu TEM grids and observed by TEM at 300 kV under vaccum conditions at room temperature, which allowed to limit destruction of the observed tissue slice by the electron beam.

2.6. Measurement of oxidative damage

The malondialdehyde (MDA) levels were measured in blood and tissues collected on days 1, 3, 7 and 14 following inhalation and compared to values in controls to obtain an indication of lipid peroxidation. The thiobarbituric acid reacting substances (TBARS) assay described in Ohkawa et al. (1979) was used. Difference in mean values between the exposed and control groups was calculated using the Student's *t*-test. The level of significance was set at $p \leq 0.05$.

3. Results and discussion

3.1. Inhalation exposure of animals

As a first step, a TiO_2 aerosol was generated in a specialized inhalation unit to expose rats during 6 continuous hours, a scenario typical of a daily worker exposure. For this purpose, a wet nebulization system was used and adapted to produce fine and stable aerosols suitable for our animal exposure. The choice of the exposure method is important because it strongly impacts on the characteristics of the aerosol generated (Schmoll et al., 2009). In a previous study, we have reported the parameters associated with this method; the system used was able to produce small

aggregates/agglomerates (<100 nm) and stable concentrations (between 0.5 and 30 mg/m^3) representative of real life exposure in occupational settings (Pujalté et al., submitted).

The microstructural analysis of the TiO_2 nanopowder by SEM (Fig. 1A) showed the agglomeration of particles in a cauliflower structure of about 3 μm. TEM analysis of the nanopowder along with the corresponding selected area electron diffraction (SAD) (Fig. 1B) showed particles having dimensions between 10 and 30 nm, as expected, and strong clusters having dimensions of hundred of nanometers to several microns. As confirmed by SAD, TiO_2 particles had a square prism shape (tetragonal shape) and the crystal structure typical of anatase with a = 3.78 Å and b = 9.51 Å. The ring shape of the diffraction pattern around the central beam is due to the nanometrical dimensions of particles. Furthermore, Fig. 1C depicts the image of a cluster of NPs dispersed in the aerosol and collected on the TEM grids; the dimension of the particles was between 10 and 30 nm as in the original powder and it was confirmed that the NPs in the aerosol had the crystallographic structure and morphology of anatase TiO_2. It was also observed that the position of the TEM grid in the inhalation chamber did not influence the microstructural characteristics of TiO_2 NPs. In general, NPs were agglomerated into clusters with sizes between hundreds of nanometers and several microns. It is important to underline that the agglomeration level of NPs on TEM grids is higher than that in the aerosol because of the natural behavior of NPs to cluster together. Therefore, it does not correspond to the agglomeration level of NPs inhaled by animals in the "nose-only" exposure chamber.

It was also verified that, during exposure, an average concentration of 15.6 mg/m^3 in the aerosol was continuously generated, which is close to the target value of 15 mg/m^3 aimed *a priori* (Table 1). Aerosol concentrations remained stable over the entire exposure period, with a mean particle numbers ±standard deviation (SD) of 665,000 ± 26,000 particles/cm^3 and a low coefficient of variation of 3.9% over 6 h (Fig. 1D). Moreover, the aerosol generated showed a monodisperse and homogenous size distribution, with a small geometric mean diameter of 76.9 and a small geometric standard deviation of 1.87 (Fig. 1E). Although, the particle size distribution in the aerosol differed from the initial particle size in the nano-power (10–30 nm), average values were below 100 nm allowing particles to access the deep lung (between 10 and 100 nm) (Kreyling, 2013). Particles with an aerodymic diameters below 10 nm have been shown to mainly deposit in the tracheobronchial region, and those with values beyond 100 nm have been recovered primarily in the head airways region (Carvalho et al., 2011; Tsuda et al., 2013). In some studies, rat exposures to aerosols with aggregated/agglomerated particles have induced effects that may be associated with non-nanosized aggregates/agglomerates (>100 nm), which significantly reduces their capacity to reach the alveolus. For example, Lindberg et al. (2012) exposed rats to TiO_2 NPs of 21 nm by inhalation, but aerosols generated NP aggregates/agglomerates of about 144 nm that could

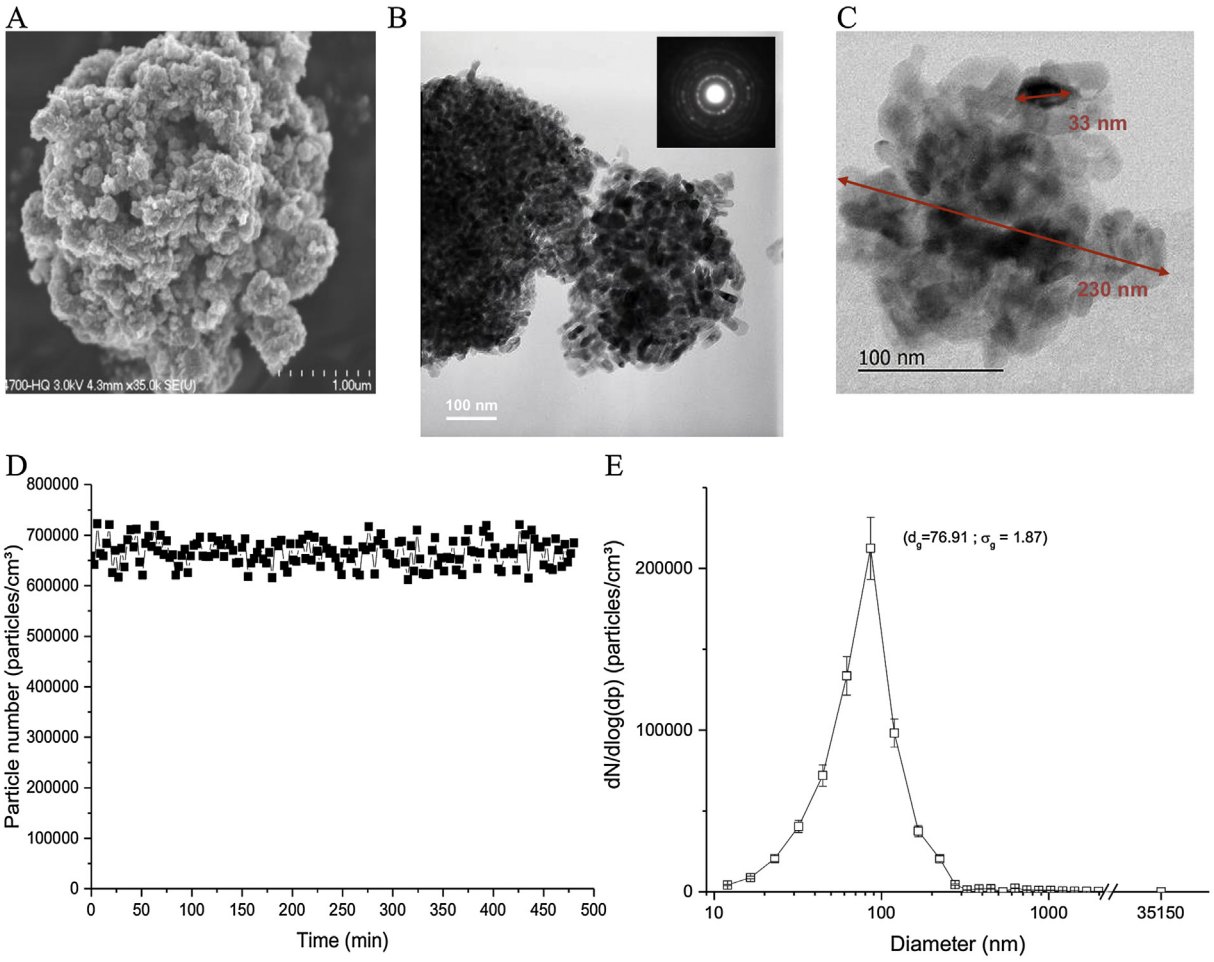

Fig. 1. (A) SEM image by secondary electrons of a cauliflower cluster of TiO_2 NPs in the nanopowder; (B) TEM image of an agglomeration of TiO_2 NPs of size between 10 and 30 nm in the nanopowder, along with the corresponding selected area electron diffraction patterns showing the typical TiO_2 anatase diffraction rings; (C) TEM image of a cluster of NPs in the aerosol produced by collision-jet method and collected on the TEM grid. (D, E) Characteristics of the aerosol generated during the 6-h inhalation exposure in male Sprague-Dawley rats: stability of particle number (particles/cm^3) in the aerosol through time (D) and granulometric size distribution of TiO_2 aerosol (nm) (E).

Table 1
Experimental conditions during inhalation exposure to TiO_2 NPs in rats and during control exposure to filtered air only.

Exposure conditions		Controls exposed to filtered air	Rats exposed to TiO_2
Concentration (mg/m^3)	Mean (min-max)	0.01 (0.005–0.018)	15.57 (9–21)
Number of particles (p/cm^3)	Mean ± SD	4748 ± 1796	665 000 ± 26 000
Particle size (nm)	Geometric mean		76.91
	Geometric standard deviation		1.87
Temperature (°C)	Mean ± SD	22.88 ± 1.6	23.04 ± 1.84
Humidity (%)	Mean ± SD	35.7 ± 4.5	43.4 ± 5.22
Pressure (mbar)	Mean ± SD	−0.15 ± 0.2	−0.17 ± 0.13
O_2 (%)	Mean ± SD	19.7 ± 0.45	19.96 ± 0.25
CO_2 (%)	Mean ± SD	0.24 ± 0.11	0.39 ± 0.21

induce a different biological reactivity (toxicity, deposition site, deposited amounts) compared to non-agglomerated NPs of 21 nm. In our study, this effect was reduced with an optimized aerosol system; fine aerosols were generated using compressed air at high velocity, and separation compartments allowing to break down and discard of large aggregates/agglomerates forming in the aerosol prior to entering the rat exposure unit.

In the inhalation exposure unit, animals were exposed "nose-only", which allowed to limit indirect exposure by ingestion, or ocular and pelt contamination (Henry et al., 1985). An acclimatation period in the exposure chamber was performed over several days prior to exposure to reduce stress in animals. Most inhalation studies on TiO_2 NPs were performed to date by whole body exposure (Baisch et al., 2014; Grassian et al., 2007). Our exposure conditions were also favorable and stable for rat exposure with a temperature of 23.0 ± 1.9 °C, humidity of 43 ± 5%, pressure of −0.2 mBar, and O_2 and CO_2 values of 20 and 0.4% (Table 1). After exposure, none of the rats died or showed signs of dyspnea or abnormal behavior (grooming, exploration, and food recovery) and no significant weight loss was observed.

3.2. Deposition, retention and clearance of TiO_2 from the lungs

Over the course of the 6-h inhalation period of TiO_2 NPs in rats and in the 14 following days, lung deposition, retention and elimination of TiO_2 were assessed. As expected, highest tissue levels were observed in the lungs. During the exposure period, amounts of TiO_2 in lungs progressively increased, reaching average values (±SD) of 945 ± 489 and 2581 ± 773 ng of TiO_2, at 3 and 6 h following exposure onset, respectively (Fig. 2A). Maximum amounts were however only reached at 48 h, with a mean (± SD) value of 3623 ± 633 ng of TiO_2. Based on total amounts of Ti found in lungs, with respect to average exposure concentration and estimated inhaled volume during the experiment (Bide et al., 2000; Kuethe et al., 2002), the average (±SD) fraction of inhaled TiO_2 dose retained in the lungs was estimated at 0.23 ± 0.13,

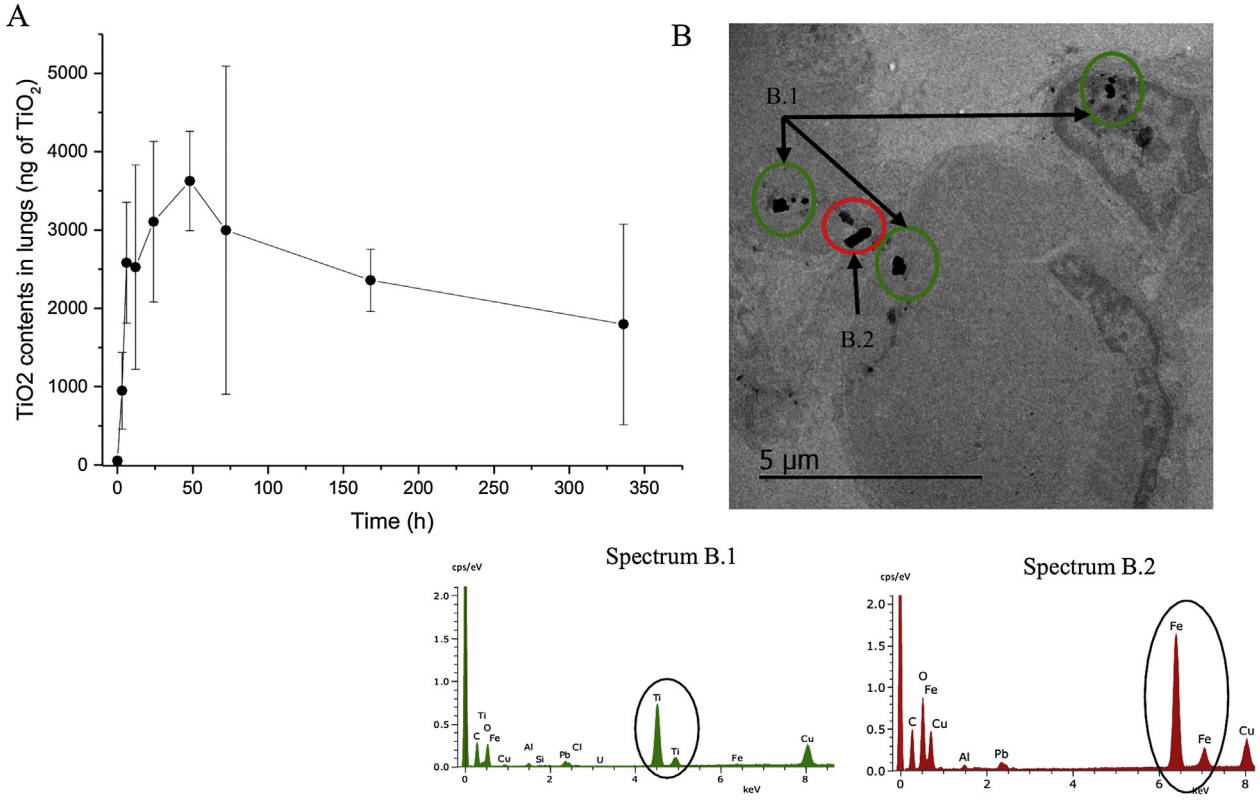

Fig. 2. Time courses of TiO_2 (ng) in lungs (A) over 336 h following the onset of a 6-h inhalation to 15 mg/m^3 of TiO_2 NPs (20-nm average diameter) in male Sprague-Dawley rats (n = 6 except the first 3 times where n = 4). Symbols represent mean values and vertical bars are standard deviations. (B) TEM image of a region of the caudal section of rat lung. EDX microanalysis of particles/clusters observed in the caudal section: spectrum B.1 shows Ti in inclusions indicated by arrows; spectrum B.2 shows Fe in the cluster indicated by the corresponding arrow.

0.33 ± 0.12 and 0.53 ± 0.36%, respectively, 3, 6 and 48 h following the onset of exposure. Amounts in total lungs thus remained relatively high over the entire assessment period, with values of 1794 ± 1279 ng of TiO_2 measured on day 14. The fact that peak levels in the lungs were observed only 48 h following the onset of the 6-h inhalation exposure to NP aerosols in rats could be explained by an initial deposition of particles by impaction and transient retention in the upper respiratory tract (naso-pharynx and larynx), in line with Tsuda et al. (2013) who detailed the importance of geometry and fluid mechanics in particle transport and deposition in the nasal, pharyngeal and laryngeal regions. The retained NPs in the upper respiratory tract could eventually reach

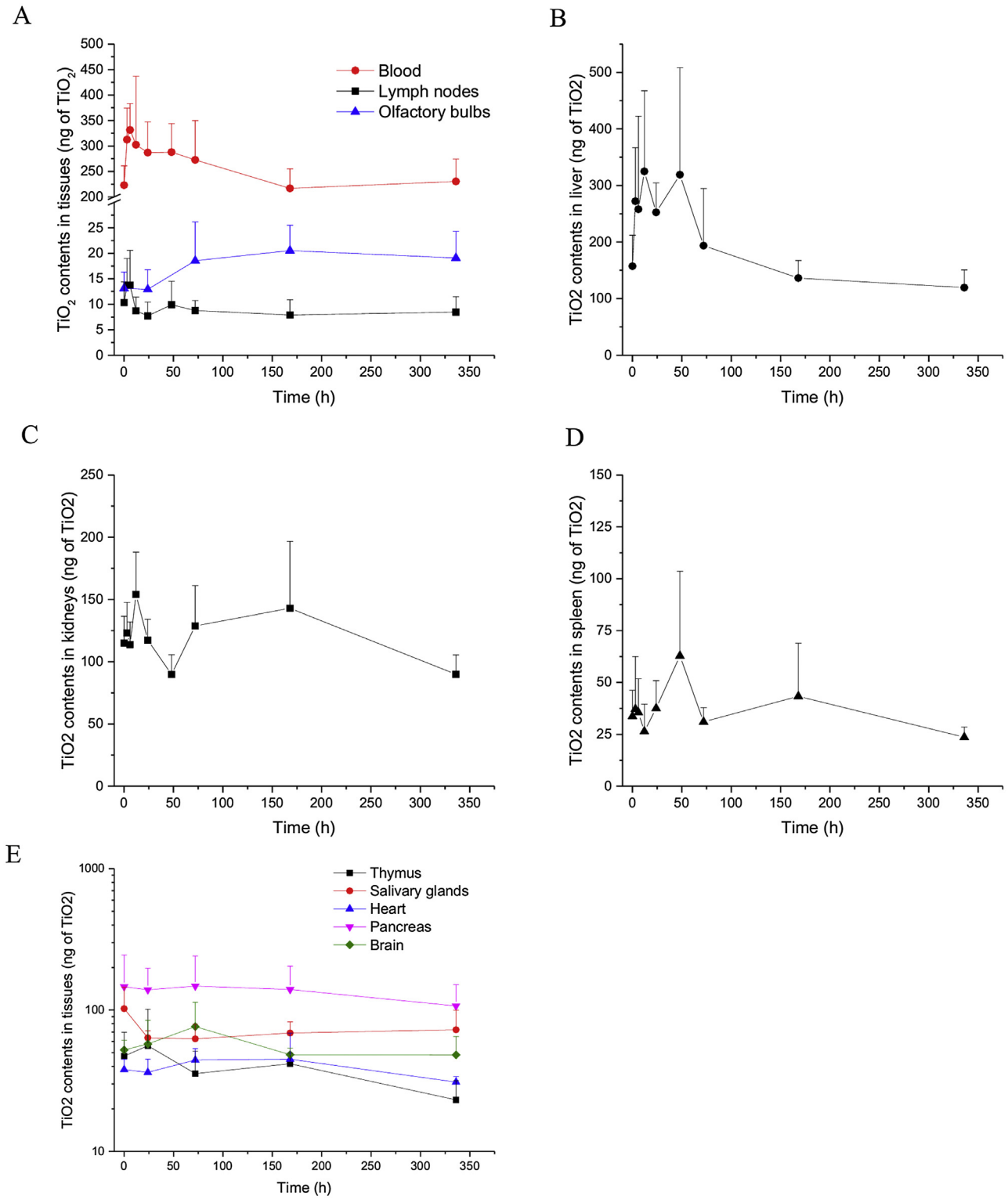

Fig. 3. Time courses of TiO_2 (ng) in blood, lymph nodes and olfactory bulbs (A) liver (B), kidneys (C), spleen (D), and thymus, salivary glands, heart, pancreas and brain (E) over 336 h following the onset of a 6-h inhalation to 15 mg/m^3 of TiO_2 NPs (20 nm of diameter) in male Sprague-Dawley rats (n = 6 except the first 3 times where n = 4). Symbols represent mean values and vertical bars are standard deviations.

lower respiratory tract regions, including the lung, which would lead to a late exposure of the lungs several hours after the end of the inhalation period. It has also been reported that deposited NPs can be retained in epithelial cells, endothelial cells and interstitial tissues (Geiser et al., 2005; Kreyling, 2013). A large part of the particles in the aerosol appears to be stopped by the upper respiratory tract mucus and then eliminated by ingestion; a large part of particles recovered in feces thus originates from their ingestion during the initial NP aerosol exposure. NPs that reach the alveolar lumen and interstitial tissues have also been documented to be predominantly cleared by alveolar macrophage mediation toward the mucociliary escalator back to the upper respiratory tract where they can be swallowed and excreted into feces (Kreyling et al., 2002; Semmler-Behnke et al., 2008). Moreover, the possible gut absorption of NPs present in the GI tract was considered negligible according to Kreyling et al. (2009). Wang et al. (2007) also showed that the translocation rate accross the GI tract epithelium was less than 0.005% of the ingested dose. Overall, our study showed a high retention and slow elimination of TiO_2 from the lungs, favoring a longer-residence time in this tissue and hence prolonged potential for translocation to the systemic circulation over time.

TEM observations of thin slices of apical, central and caudal sections of rat lungs coupled to EDX microanalysis (carried out to understand the chemical composition of particles and clusters in these biological sections) did not reveal any presence of Ti in the central and apical sections. Ti NPs were observed only during the investigation of caudal sections. Fig. 2B shows a typical image of a caudal section of a lung indicating the presence of two groups of particles having a composition rich in Ti. Particles formed clusters having dimensions between 100 nm and 400 nm. As revealed from the image, the electron beam was focused on the region just around each cluster. It is to be noted that, in every EDX spectrum, there is always an instrumental/preparation contribution to the observed elements, because of the sample holder (Al and Si), the TEM grid (Cu) and the sample preparation (Pb, U, Os and Cl). Spectrum B.1 clearly depicts the presence of Ti while spectrum B.2 shows the presence of Fe in the rectangular agglomeration (size of 200 nm × 680 nm); the source of this Fe has not been identified.

3.3. Translocation to the body

Translocation to blood and lymph nodes was assessed. As shown in Fig. 3A, a slight increase of TiO_2 amounts in blood was observed during the 6-h inhalation period. Peak levels in blood appeared to be reached at 12 h following the onset of exposure with average values (±SD) of 331 ± 52 ng of TiO_2. Levels slowly decreased thereafter and returned to baseline values after seven days. The time course of TiO_2 in lymph nodes (Fig. 3A) also revealed a slight increase in TiO_2 levels during the 6-h inhalation period with values returning to baseline levels after 12 h. These observed time courses did not allow to clearly define toxicokinetic parameter values. The lymph nodes have been described as the primary target of NPs after lung translocation (Choi et al., 2010; Kreyling et al., 2010), but our study, like other published studies, failed to differentiate between direct transport of NPs into the interstitium and then the blood, and transport through lymphatic circulation to blood. Further investigations are necessary to understand this mechanism. Nonetheless, with the exposure conditions used, the translocation rate of TiO_2 NPs to the lymphatic system and the blood circulation was found to be low compared to total amounts of NPs retained in the lungs through time. Other mechanisms, such as alveolar macrophage phagocytosis of NPs, mucociliary transport of macrophage-associated NPs toward the GI tract and ensuing ingestion, appear to contribute to a greater extent to the elimination of inhaled NPs (Braakhuis et al., 2014; Geiser, 2010; Geiser and Kreyling, 2010).

3.4. Transport to the brain and olfactory bulbs

The brain was also reported as a target of NPs after inhalation; small NPs in the nasal cavity have been suggested to be able to be transported by axonal transport through the nasal nerve to the olfactory bulbs and brain (Simkó and Mattsson, 2010). In our study, a slight increase in TiO_2 levels in olfactory bulbs (Fig. 3A) and brain (Fig. 3E) was visually apparent following inhalation with a peak at 72 h. Chen et al. (2006) have also detected Ti contents in the sub-brain regions (olfactory bulb, cerebral cortex, hippocampus and cerebellum) after nasal instillation of TiO_2 NPs in rats. These data indicate a potential for translocation and accumulation of TiO_2 NPs in the brain following repeated exposure. Our study does not differentiate between NPs translocated directly from the nasal area to the brain and the lung fraction reaching the bloodstream or lymphatic system and in turn the brain after crossing the hemato-encephalic barrier. The delay in peak levels of NPs in the latter tissues compared to other internal organs may suggest a translocation mechanism different from the one observed in other organs (Fig. 3B–D). Future research is needed to understand the translocation mechanisms and evaluate possible neurotoxic effects.

3.5. Distribution in other tissues

Lung translocation to blood is considered as the most important gateway to the systemic circulation and deep organs. After the lung, highest tissue levels were found in the liver, followed by the kidneys as depicted in Fig. 3B and C. A slight increase in mean levels was apparent post-inhalation in these tissues, with peak values observed at 12–48 h, followed by a progressive decrease over the course of the 14-day assessment. However, levels were highly variable through time and did not allow to determine toxicokinetic parameters. The presence of NPs in these organs was also reported following intravenous injection. In the study of Elgrabli et al. (2015), the majority of injected TiO_2 was recovered in the liver, spleen and kidneys, which can be explained by the high vascularization of these organs. These levels reflect the active role of the liver and kidneys in the clearance of TiO_2 from the systemic circulation. Uptake of NPs by liver Kupffer and endothelial

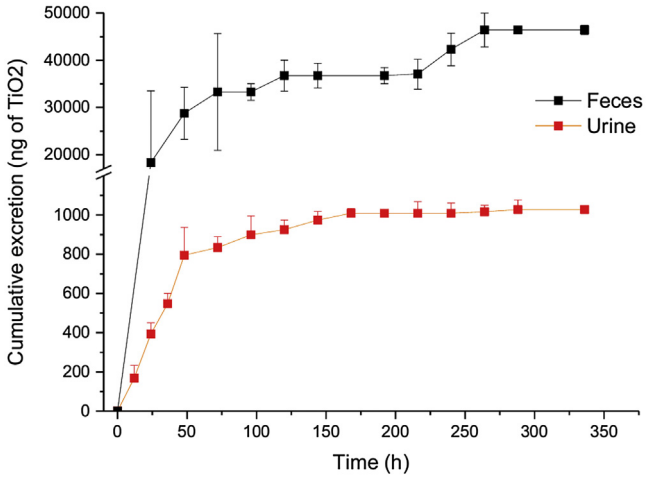

Fig. 4. Cumulative excretion time profiles of TiO_2 (ng) in urine and feces over 336 h following the onset of a 6-h inhalation to 15 mg/m^3 of TiO_2 NPs (20 nm of diameter) in male Sprague-Dawley rats (n = 6 except the first 3 times where n = 4). Symbols represent mean values and vertical bars are standard deviations.

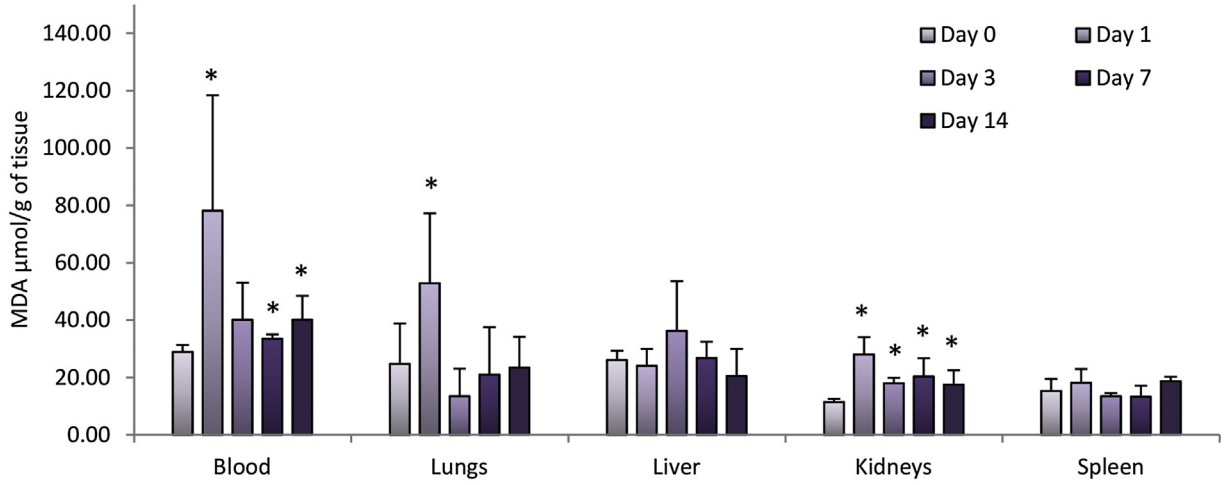

Fig. 5. Malondialdehyde contents in blood, lung, liver, kidney and spleen over 336 h following the onset of a 6 h inhalation to 15 mg/m^3 of TiO_2 NPs (20 nm of diameter) in male Sprague-Dawley rats (n = 6). Each value represents mean and vertical bars are standard deviations. Student's *t*-test for unpaired samples: controls vs exposed rats. *P < 0.05.

cells have been documented *in vivo* in rats (Lenaerts et al., 1984; Sadauskas et al., 2007). Uptake of NPs by renal proximal tubular cells and mesangial cells and their presence in the extracellular matrix have also been reported (Choi et al., 2011 Pujalté et al., 2011). For the other organs, thymus, salivary glands, pancreas and heart, amounts were relatively constant through time and lower than in lungs, liver and kidneys (Fig. 3E).

3.6. Excretion

The cumulative excretion of TiO_2 in urine and feces over 14 days following inhalation of TiO_2 NPs shows that TiO_2 is mainly excreted in feces, with values respectively reaching and 1027 and 46 414 ng (Fig. 4). Again, these data combined to the observed time courses of TiO_2 in lung, blood and lymph nodes are compatible with a mucociliary clearance from the respiratory tract and ensuing ingestion of NPs (Kreyling et al., 2002; Semmler-Behnke et al., 2008). TiO_2 present in blood is also eliminated in liver and in turn feces mainly according to kinetic data in intravenously exposed rats (Xie et al., 2011). Nonetheless, this contribution cannot be assessed following inhalation given the proportionally much lower TiO_2 values observed in blood and liver compared to lungs, the latter contributing to the majority of TiO_2 amounts recovered in feces. A certain translocation of TiO_2 NPs from blood to urine is also apparent from the urinary time courses (Fig. 4), with the majority of TiO_2 excreted in urine over 14 days being recovered during the first 48 following the onset of inhalation.

3.7. Oxidative damage

Levels of the MDA marker of lipid peroxidation were followed in lung, blood, and the three main tissues with detectable TiO_2 (liver, kidney and spleen) over the 14-days following inhalation. At 24 h following the onset of inhalation of TiO_2 NPs, MDA levels in lungs and blood were significantly higher than control values ($p < 0.05$) but this was not clearly reflected at later times (Fig. 5). In kidneys, MDA levels were stable with time over the 14-days post-inhalation but slightly higher than control values. This needs to be further investigated. However, endocytosis of TiO_2 NPs and oxidative damage associated with ROS production ($HO^{\bullet}$ and $O_2^{\bullet -}$) have previously been reported in liver and kidneys after intratracheal instillation (Liang et al., 2009), in lungs after intratracheal instillation (Afaq et al., 1998), and in cultured BEAS–2 B lung cells (Park et al., 2008). The latter results indicate that oxidative damage may occur as a result of TiO_2 NP uptake in tissues. Other damages should be evaluated in lungs and blood but also in peripheral tissues (brain, liver, kidney and spleen).

4. Conclusion

In conclusion, this study provided novel data on the kinetics of TiO_2 following a 6-h inhalation of poorly agglomerated NPs of 20 nm initial diameter, typical of a worker exposure. Retention in the lungs during and following inhalation was evidenced with a poor translocation to blood and lymphatic system compared to the amounts excreted in feces, most plausibly following mucociliary clearance. Nonetheless, a certain fraction of inhaled dose appeared to be transferred into the systemic circulation and to reach secondary organs, such as the liver, kidneys and spleen, which contained detectable levels of TiO_2. The observed levels of NPs in the lungs up to 14 days following inhalation may concur to increase the rate of oxidative damage after repeated exposure. A certain translocation to the olfactory bulb and the brain was also observed; the mechanisms by which such phenomenom occurs should be further investiged.

Declaration of interest

The authors report no conflicts of interest. The authors alone are responsible for the contents and writing of the paper.

Acknowledgments

This study was funded by NanoQuebec (now PrimaQuebec), the Institute of Research of Hydro-Quebec, and the Institut de recherche en santé publique de lU'niversité de Montréal (IRSPUM), Canada. This study was also partly funded by the Chair in Toxicological risk Assessment and Management of the University of Montreal, Canada.

References

Afaq, F., Abidi, P., Matin, R., Rahman, Q., 1998. Cytotoxicity, pro-oxidant effects and antioxidant depletion in rat lung alveolar macrophages exposed to ultrafine titanium dioxide. J. Appl. Toxicol. 18, 307–312.

Baisch, B.L., Corson, N.M., Wade-Mercer, P., Gelein, R., Kennell, A.J., Oberdorster, G., Elder, A., 2014. Equivalent titanium dioxide nanoparticle deposition by intratracheal instillation and whole body inhalation: the effect of dose rate on acute respiratory tract inflammation. Part Fibre Toxicol. 11, b5.

Berges, M.G., 2013. 1.2 exposure during production and handling of manufactured nanomaterials. Commission for the Investigation of Health Hazards of Chemical Compounds in the Work Area, , pp. 25.
Bermudez, E., Mangum, J.B., Asgharian, B., Wong, B.A., Reverdy, E.E., Janszen, D.B., Hext, P.M., Warheit, D.B., Everitt, J.I., 2002. Long-term pulmonary responses of three laboratory rodent species to subchronic inhalation of pigmentary titanium dioxide particles. Toxicol. Sci. 70, 86–97.
Berube, D.M., Searson, E.M., Morton, T.S., Cummings, C.L., 2010. Project on emerging nanotechnologies-consumer product inventory evaluated. Nanotech. Law Bus. 7, 152.
Bide, R., Armour, S., Yee, E., 2000. Allometric respiration/body mass data for animals to be used for estimates of inhalation toxicity to young adult humans. J. Appl. Toxicol. 20, 273–290.
Braakhuis, H.M., Park, M., Gosens, I., De Jong, W.H., Cassee, F.R., 2014. Physicochemical characteristics of nanomaterials that affect pulmonary inflammation. Part Fibre Toxicol. 11, 18.
Carvalho, T.C., Peters, J.I., Williams III, R.O., 2011. Influence of particle size on regional lung deposition —What evidence is there? Int. J. Pharmaceut 406, 1–10.
Chen, J., Tan, M., Nemmar, A., Song, W., Dong, M., Zhang, G., Li, Y., 2006. Quantification of extrapulmonary translocation of intratracheal-instilled particles in vivo in rats: effect of lipopolysaccharide. Toxicology 222, 195–201.
Chen, J., Dong, X., Zhao, J., Tang, G., 2009. In vivo acute toxicity of titanium dioxide nanoparticles to mice after intraperitioneal injection. J. Appl. Toxicol. 29, 330–337.
Choi, H.S., Ashitate, Y., Lee, J.H., Kim, S.H., Matsui, A., Insin, N., Bawendi, M.G., Semmler-Behnke, M., Frangioni, J.V., Tsuda, A., 2010. Rapid translocation of nanoparticles from the lung airspaces to the body. Nat. Biotechnol. 28, 1300–1303.
Choi, C.H.J., Zuckerman, J.E., Webster, P., Davis, M.E., 2011. Targeting kidney mesangium by nanoparticles of defined size. Proc. Natl. Acad. Sci. U. S. A. 108, 6656–6661.
Driscoll, K.E., Costa, D.L., Hatch, G., Henderson, R., Oberdorster, G., Salem, H., Schlesinger, R.B., 2000. Intratracheal instillation as an exposure technique for the evaluation of respiratory tract toxicity: uses and limitations. Toxicol. Sci. 55, 24–35.
Elgrabli, D., Beaudouin, R., Jbilou, N., Floriani, M., Pery, A., Rogerieux, F., Lacroix, G., 2015. Biodistribution and clearance of TiO2 nanoparticles in rats after intravenous injection. PLoS One 10, e0124490.
Geiser, M., Kreyling, W.G., 2010. Deposition and biokinetics of inhaled nanoparticles. Part Fibre Toxicol. 7, 1–17.
Geiser, M., Rothen-Rutishauser, B., Kapp, N., Schürch, S., Kreyling, W., Schulz, H., Semmler, M., Hof, V.I., Heyder, J., Gehr, P., 2005. Ultrafine particles cross cellular membranes by nonphagocytic mechanisms in lungs and in cultured cells. Environ. Health Persp. 1555–1560.
Geiser, M., 2010. Update on macrophage clearance of inhaled micro-and nanoparticles. J. Aerosol Med. Pulm.y Drug Deliv. 23, 207–217.
Grassian, V.H., O'Shaughnessy, P.T., Adamcakova-Dodd, A., Pettibone, J.M., Thorne, P. S., 2007. Inhalation exposure study of titanium dioxide nanoparticles with a primary particle size of 2 to 5 nm. Environ. Health Persp. 397–402.
Guo, L., Liu, X., Qin, D., Gao, L., Zhang, H., Liu, J., Cui, Y., 2009. Effects of nanosized titanium dioxide on the reproductive system of male mice. Zhonghua nan ke xue = Nat. J. Androl. 15, 517–522.
Henry, C., Dansie, D., Kanagalingam, K., Kouri, R., Gayle, T., Guerin, M., Holmberg, R., Florant, L., Greenspan, J., 1985. Chronic inhalation studies in mice: I: facilities and equipment for nose-only exposure to cigarette smoke. Contrib. Tobacco Res. 13, 37–53.
Hinds, W.C., 1999. Aerosol Technology: Properties, Behavior, and Measurement of Airborne Particles. Wiley.
Iavicoli, I., Leso, V., Bergamaschi, A., 2012. Toxicological effects of titanium dioxide nanoparticles: a review of in vivo studies. J. Nanomater. 2012, 5.
Kreyling, W., Semmler, M., Erbe, F., Mayer, P., Takenaka, S., Schulz, H., Oberdörster, G., Ziesenis, A., 2002. Translocation of ultrafine insoluble iridium particles from lung epithelium to extrapulmonary organs is size dependent but very low. J. Toxicol. Environ. Health A 65, 1513–1530.
Kreyling, W.G., Semmler-Behnke, M., Seitz, J., Scymczak, W., Wenk, A., Mayer, P., Takenaka, S., Oberdörster, G., 2009. Size dependence of the translocation of inhaled iridium and carbon nanoparticle aggregates from the lung of rats to the blood and secondary target organs. Inhal. Toxicol. 21, 55–60.
Kreyling, W.G., Hirn, S., Schleh, C., 2010. Nanoparticles in the lung. Nat. Biotechnol. 28, 1275–1276.
Kreyling, W.G., 2013. Toxicokinetics of inhaled nanoparticles. Nanomaterials 32–36.
Kuethe, D.O., Behr, V.C., Begay, S., 2002. Volume of rat lungs measured throughout the respiratory cycle using 19F NMR of the inert gas SF6. Magnet. Reson. Med. 48, 547–549.
Kuhlbusch, T.A., Asbach, C., Fissan, H., Göhler, D., Stintz, M., 2011. Nanoparticle exposure at nanotechnology workplaces: a review. Part Fibre Toxicol. 8, 22.
Landsiedel, R., 2013. Studies on the inhalation uptake and effects of nanomaterials. Nanomaterials 43–48.
Lenaerts, V., Nagelkerke, J., Van Berkel, T., Couvreur, P., Grislain, L., Roland, M., Speiser, P., 1984. In vivo uptake of polyisobutyl cyanoacrylate nanoparticles by rat liver Kupffer, endothelial, and parenchymal cells. J. Pharm. Sci. 73, 980–982.
Li, N., Ma, L., Wang, J., Zheng, L., Liu, J., Duan, Y., Liu, H., Zhao, X., Wang, S., Wang, H., 2010. Interaction between nano-anatase TiO2 and liver DNA from mice in vivo. Nanoscale Res. Lett. 5, 108–115.
Liang, G., Pu, Y., Yin, L., Liu, R., Ye, B., Su, Y., Li, Y., 2009. Influence of different sizes of titanium dioxide nanoparticles on hepatic and renal functions in rats with correlation to oxidative stress. J. Toxicol. Environ. Health A 72, 740–745.
Lindberg, H.K., Falck, G.C.-M., Catalán, J., Koivisto, A.J., Suhonen, S., Järventaus, H., Rossi, E.M., Nykäsenoja, H., Peltonen, Y., Moreno, C., 2012. Genotoxicity of inhaled nanosized TiO2 in mice. Mutat. Res.-Gen. Toxicol. Environ. 745, 58–64.
Liu, H., Ma, L., Zhao, J., Liu, J., Yan, J., Ruan, J., Hong, F., 2009. Biochemical toxicity of nano-anatase TiO2 particles in mice. Biol. Trace Elem. Res. 129, 170–180.
Mester, Z., Sturgeon, R.E., 2003. Sample Preparation for Trace Element Analysis. Elsevier Science.
Noël, A., Maghni, K., Cloutier, Y., Dion, C., Wilkinson, K.J., Hallé, S., Tardif, R., Truchon, G., 2012. Effects of inhaled nano-TiO2 aerosols showing two distinct agglomeration states on rat lungs. Toxicol. Lett. 214, 109–119.
Noël, A., Charbonneau, M., Cloutier, Y., Tardif, R., Truchon, G., 2013a. Rat pulmonary responses to inhaled nano-TiO2: effect of primary particle size and agglomeration state. Part Fibre Toxicol. 10, 48.
Noël, A., Cloutier, Y., Wilkinson, K.J., Dion, C., Hallé, S., Maghni, K., Tardif, R., Truchon, G., 2013b. Generating nano-aerosols from TiO2 (5 nm) nanoparticles showing different agglomeration states. Application to toxicological studies. J. Occup. Environ. Hyg. 10, 86–96.
Ohkawa, H., Ohishi, N., Yagi, K., 1979. Assay for lipid peroxides in animal tissues by thiobarbituric acid reaction. Anal. Biochem. 95, 351–358.
Osier, M., Oberörster, G., 1997. Intratracheal inhalation vs intratracheal instillation: differences in particle effects. Toxicol. Sci. 40, 220–227.
Park, E.-J., Yi, J., Chung, K.-H., Ryu, D.-Y., Choi, J., Park, K., 2008. Oxidative stress and apoptosis induced by titanium dioxide nanoparticles in cultured BEAS-2B cells. Toxicol. Lett. 180, 222–229.
Pujalté, I., Passagne, I., Brouillaud, B., Tréguer, M., Durand, E., Ohayon-Courtès, C., L'Azou, B., 2011. Cytotoxicity and oxidative stress induced by different metallic nanoparticles on human kidney cells. Part Fibre Toxicol. 8, 1–16.
Sadauskas, E., Wallin, H., Stoltenberg, M., Vogel, U., Doering, P., Larsen, A., Danscher, G., 2007. Kupffer cells are central in the removal of nanoparticles from the organism. Part Fibre Toxicol. 4, 10.
Schmoll, L.H., Elzey, S., Grassian, V.H., O'Shaughnessy, P.T., 2009. Nanoparticle aerosol generation methods from bulk powders for inhalation exposure studies. Nanotoxicology 3, 265–275.
Semmler-Behnke, M., Kreyling, W.G., Lipka, J., Fertsch, S., Wenk, A., Takenaka, S., Schmid, G., Brandau, W., 2008. Biodistribution of 1.4-and 18-nm gold particles in rats. Small 4, 2108–2111.
Shi, H., Magaye, R., Castranova, V., Zhao, J., 2013. Titanium dioxide nanoparticles: a review of current toxicological data. Part Fibre Toxicol. 10, 15.
Simkó, M., Mattsson, M.-O., 2010. Risks from accidental exposures to engineered nanoparticles and neurological health effects: a critical review. Part Fibre Toxicol. 7, 1–8.
Subramanian, K.S., 2006. Sample preparation for elemental analysis of biological samples in the environment. Encyclopedia Anal. Chemi.y doi:http://dx.doi.org/10.1002/9780470027318.a0861.
Tsuda, A., Henry, F.S., Butler, J.P., 2013. Particle transport and deposition: basic physics of particle kinetics. Compr. Physiol. 3 (4), 1437–1471.
Wang, J., Zhou, G., Chen, C., Yu, H., Wang, T., Ma, Y., Jia, G., Gao, Y., Li, B., Sun, J., 2007. Acute toxicity and biodistribution of different sized titanium dioxide particles in mice after oral administration. Toxicol. Lett. 168, 176–185.
Xie, G., Wang, C., Sun, J., Zhong, G., 2011. Tissue distribution and excretion of intravenously administered titanium dioxide nanoparticles. Toxicol. Lett. 205, 55–61.
Yeh, H., Snipes, M., Eidson, A., Hobbs, C., Henry, M., 1990. Comparative evaluation of nose-only versus whole-body inhalation exposures for rats—Aerosol characteristics and lung deposition. Inhal. Toxicol. 2, 205–221.
Zhao, J., Li, N., Wang, S., Zhao, X., Wang, J., Yan, J., Ruan, J., Wang, H., Hong, F., 2010. The mechanism of oxidative damage in the nephrotoxicity of mice caused by nano-anatase TiO2. J. Exp. Nanosci. 5, 447–462.